Inorganic Chemistry

ARTICLE

pubs.acs.org/IC

Silylation of the Uranyl Ion Using $B(C_6F_5)_3$-Activated Et_3SiH

David D. Schnaars, Guang Wu, and Trevor W. Hayton*

Department of Chemistry and Biochemistry, University of California Santa Barbara, Santa Barbara, California 93106, United States

Supporting Information

ABSTRACT: Addition of 2 equiv of $HSiEt_3$ to $UO_2(^{Ar}acnac)_2$ ($^{Ar}acnac$ = Ar*N*C(Ph)CHC(Ph)*O*, Ar = 3,5-$^tBu_2C_6H_3$) in the presence of 1 equiv of $B(C_6F_5)_3$ results in formation of the U(V) bis(silyloxide) complex $[U(OSiEt_3)_2(^{Ar}acnac)_2][HB(C_6F_5)_3]$ (**1**) in 80% yield. Also produced in the reaction, as a minor product, is $U(OSiEt_3)(OB\{C_6F_5\}_3)(^{Ar}acnac)_2$ (**2**). Interestingly, thermolysis of **1** at 85 °C for 24 h also results in formation of **2**, concomitant with production of Et_3SiH. Addition of 1 equiv of Cp_2Co to **1** results in formation of $U(OSiEt_3)_2(^{Ar}acnac)_2$ (**3**) and $[Cp_2Co][HB(C_6F_5)_3]$ (**4**), which can be isolated in 61% and 71% yields, respectively. Complexes **1**−**3** have been characterized by X-ray crystallography, while the solution-phase redox properties of **1** have been measured with cyclic voltammetry.

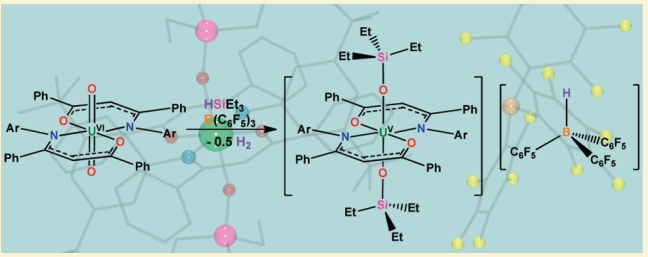

INTRODUCTION

Oxo ligand functionalization of the uranyl ion (UO_2^{2+}) has proven a challenge,[1] due in part to the strength of the oxygen−uranium interaction within the UO_2^{2+} fragment. For example, the mean U−O bond dissociation energy of uranyl (604 kJ/mol)[2] is 72 kJ/mol larger than that observed for CO_2 (532 kJ/mol).[3] The challenge of perturbing the uranyl moiety is well illustrated by reaction of UO_3 with neat triflic acid at 110 °C.[4,5] Under these conditions, only one oxo group in UO_3 is protonated, providing $UO_2(OTf)_2$ and H_2O. Even in this extremely acidic environment the uranyl moiety remains intact, and no evidence for protonation of the remaining oxo ligands is observed.

Despite these difficulties and motivated by the importance of uranyl in the nuclear fuel cycle,[6−11] interest in discovering chemical strategies for functionalizing this extremely stable fragment has grown in recent years. For example, uranyl oxo ligand metalation can be achieved by reaction of $UO_2(THF)(H_2L)$ (L = 'Pacman' polypyrrolic macrocycle) with a variety of lithium reagents[12] or rare earth silylamides.[13] Likewise, Mazzanti and co-workers observed oxo metalation in a series of uranyl(V) β-ketonate and Schiff base complexes.[14−20] In addition, several laboratories have been investigating uranyl oxo ligand functionalization via reductive silylation.[21−28] This transformation was first observed by Ephritikhine and co-workers through the reaction of excess Me_3SiX (X = Cl, Br, I) with $UO_2I_2(THF)_3$ in MeCN. This results in formation of the U(IV) halide complexes $UX_4(MeCN)_4$ in good yields.[24] Although not observed in the reaction mixture, the oxygen atoms of the uranyl fragment are likely converted into $Me_3SiOSiMe_3$.[22] More recently, the Arnold group demonstrated that deprotonation of $UO_2(THF)(H_2L)$, followed by addition of silylamine, resulted in generation of a U(V) silyloxide $[UO(OSiMe_3)(THF)Fe_2I_2L]$.[25−28] In a similar example recently reported by our group,[23] the synthesis of $U(OSiPh_3)(OB\{C_6F_5\}_3)(^{Ar}acnac)_2$ was achieved by reductive silylation of $UO_2(^{Ar}acnac)_2$ ($^{Ar}acnac$ = Ar*N*C(Ph)CHC(Ph)*O*, Ar = 3,5-$^tBu_2C_6H_3$) using a combination of $HSiPh_3$ and $B(C_6F_5)_3$.[23] We argued that the reaction proceeded by formation of a borane−silane adduct, $[Ph_3SiH\cdots B(C_6F_5)_3]$.[29−31] The activated silane was then attacked by the uranyl oxo, resulting in Si−O bond formation and eventual generation of $U^V(OSiPh_3)(OB\{C_6F_5\}_3)(^{Ar}acnac)_2$ and 0.5 equiv of H_2. While $B(C_6F_5)_3$-mediated hydrosilylation is known for a variety of organic substrates,[29,32−36] to our knowledge this was the first reported example of borane-mediated silylation of a metal oxo complex. Herein, we report a second example of $B(C_6F_5)_3$-mediated silylation of the uranyl oxo fragment, concomitant with reduction to U(V), and provide further insight into the mechanism of this transformation.

RESULTS AND DISCUSSION

To expand the scope of borane-mediated silylation of uranyl,[23] we explored the reactivity of the $UO_2(^{Ar}acnac)_2/B(C_6F_5)_3$ system with $HSiEt_3$. Thus, addition of 2 equiv of $HSiEt_3$ to $UO_2(^{Ar}acnac)_2$, in the presence of $B(C_6F_5)_3$, results in formation of a deep red solution, from which $[U(OSiEt_3)_2(^{Ar}acnac)_2][HB(C_6F_5)_3]$ (**1**) can be isolated as a dark red crystalline material in 80% yield (Scheme 1).

Complex **1** crystallizes in the triclinic space group $P\bar{1}$ as a discrete cation/anion pair (Figure 1). There are two crystallographically unique $[U(OSiEt_3)_2(^{Ar}acnac)_2]^+$ cations within the asymmetric unit, each sitting on a special position. The metrical parameters of both cations are similar, and only one will be discussed in detail. The uranium center in **1** is coordinated by two triethylsilyloxide ligands oriented is trans arrangement, while two $^{Ar}acnac$ ligands occupy the equatorial plane. The $U-O_{Si}$ and O−Si bond

Received: June 28, 2011
Published: August 15, 2011

Scheme 1

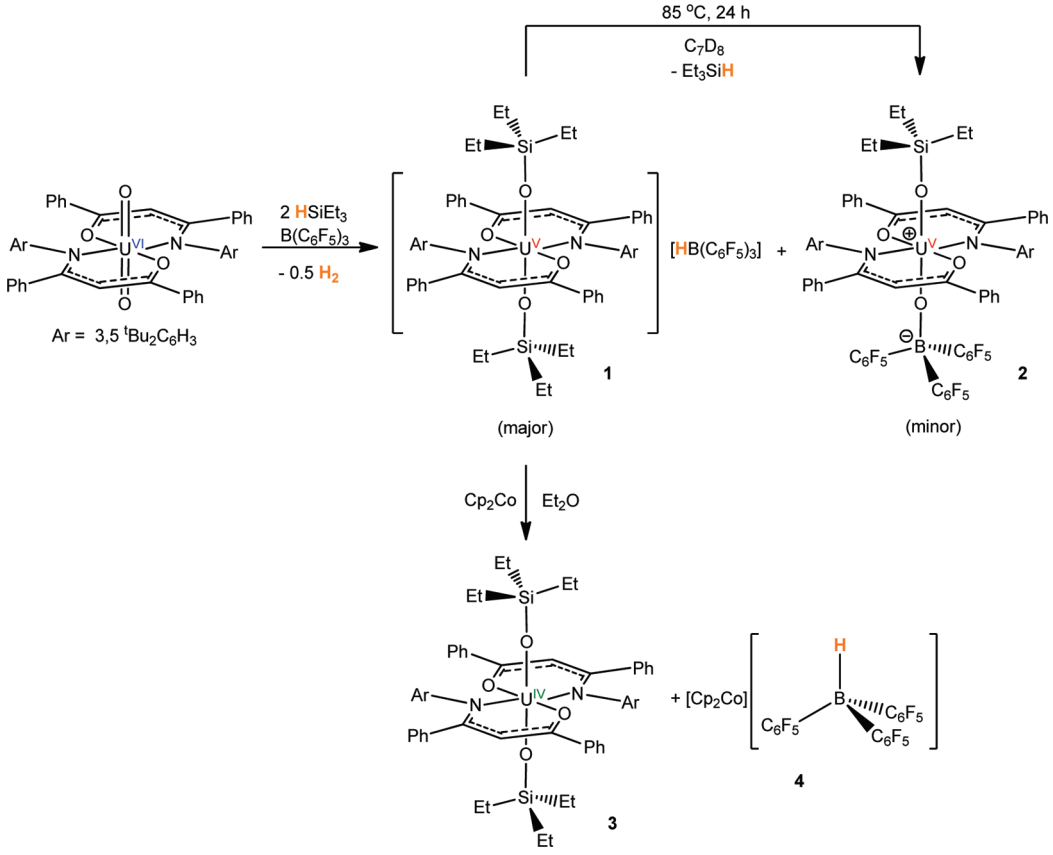

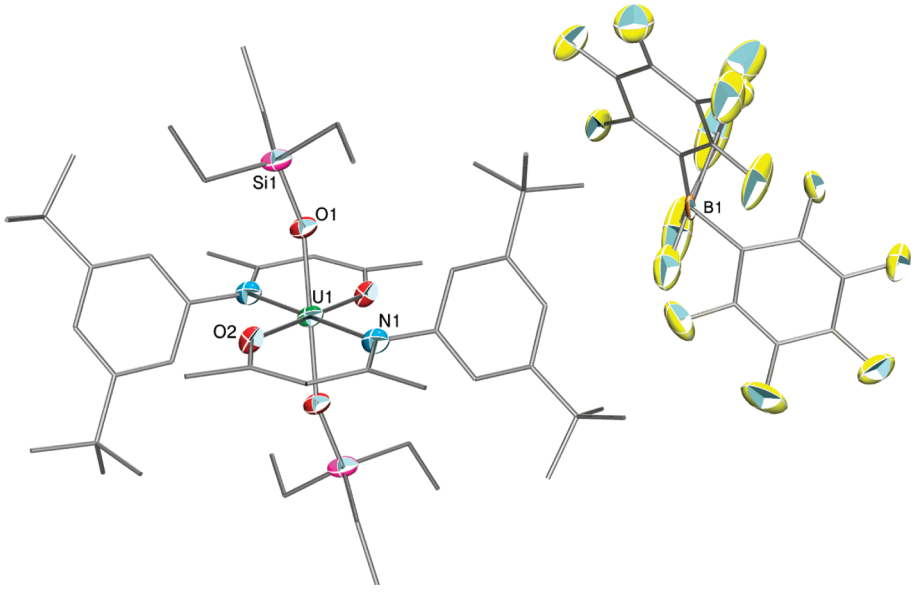

Figure 1. Solid-state structure of $[U(OSiEt_3)_2(^{Ar}acnac)_2][HB(C_6F_5)_3]$ (**1**) with 50% probability ellipsoids for the noncarbon atoms. The phenyl rings on the ^{Ar}acnac backbone have been removed for clarity.

lengths are 2.011(4) and 1.678(4) Å, respectively, while the U−N and U−O_{acnac} bond lengths are 2.383(5) and 2.171(4) Å, respectively (Table 1). Overall, these metrical parameters are similar to those of the previously characterized U(V) silyloxide $U(OSiPh_3)(OB\{C_6F_5\}_3)(^{Ar}acnac)_2$.[23] The metrical parameters of the $[HB(C_6F_5)_3]^-$ anion are also similar to those observed previously.[37,38] However, it should be noted the $[HB(C_6F_5)_3]^-$ moiety in **1** was found to be disordered over two positions in a 65:35 ratio.

dx.doi.org/10.1021/ic201385h |*Inorg. Chem.* 2011, 50, 9642–9649

The room-temperature ^{1}H NMR spectrum of **1** in CD_2Cl_2 is consistent with the proposed formulation and, as observed for $U(OSiPh_3)(OB\{C_6F_5\}_3)(^{Ar}acnac)_2$,[23] reveals the presence of major and minor isomers in solution in a 9:1 ratio. For example, a resonance at −0.05 ppm is attributable to the ^{t}Bu substituents of the major isomer, while the corresponding resonances for the minor isomer are observed as two overlapping signals at −0.40 ppm. These latter signals separate upon cooling to 12 °C, where they are observed at −0.42 and −0.48 ppm. The observation of two ^{t}Bu environments for the minor isomer of **1** can be explained by invoking a cis configuration of the two silyloxide groups and assuming that rotation about the N−C_{ipso} bond of the ^{Ar}acnac ligand is hindered (eq 1). In addition, the ^{19}F spectrum of **1** consists of three sharp resonances at −69.80, −100.63, and −103.46 ppm in a 2:1:2 ratio, respectively, corresponding to the ortho, para, and meta environments of the $[HB(C_6F_5)_3]^-$ anion.[35,37−40] The solid state IR spectrum of **1** features a broad ν_{BH} absorption at 2377 cm^{-1}, further supporting the presence of $[HB(C_6F_5)_3]^-$ anion.[41−43] Finally, the NIR spectrum of **1** is similar to that observed for other U(V) complexes, corroborating the presence of a $5f^1$ ion (Figure 2).[21,23,44−46]

Table 1. Selected Bond Lengths (Å) and Angles (deg) for Complexes 1−3

	1	2	3
U−O_{Si}	2.011(4)	2.017(6)	2.129(2)
U−O_B		1.957(6)	
U−O_{acnac}	2.171(4)	2.165(7)	2.268(2)
		2.198(6)	
U−N	2.383(5)	2.440(7)	2.484(3)
		2.446(7)	
O−Si	1.678(4)	1.664(7)	1.628(2)
O−B		1.525(12)	
∠O−U−O	180	175.0(3)	180
∠U−O−Si	161.5(3)	168.0(4)	158.96(15)
∠U−O−B		166.6(6)	

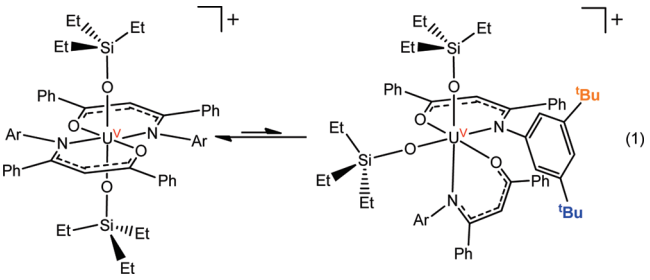

(1)

We also monitored the in situ reaction of $UO_2(^{Ar}acnac)_2$ with 1 equiv of $B(C_6F_5)_3$ and 2 equiv of $HSiEt_3$ in C_6D_6 over the course of 21 h using ^{1}H and ^{19}F NMR spectroscopies. Under these conditions, complex **1** is the major product. However, a minor side product is also observed in the reaction mixture, which we identified as $U(OSiEt_3)(OB\{C_6F_5\}_3)(^{Ar}acnac)_2$ (**2**), the triethylsilyl analogue of the previously reported $U(OSiPh_3)(OB\{C_6F_5\}_3)(^{Ar}acnac)_2$ (Scheme 1).[23] Complexes **1** and **2** are observed in a 4:1 ratio, respectively. Complex **2** can be identified by its characteristic CH_2CH_3 resonance at 3.41 ppm, which is downfield from the corresponding resonance in **1** (Figures S17−S18, Supporting Information). The ^{1}H NMR spectrum

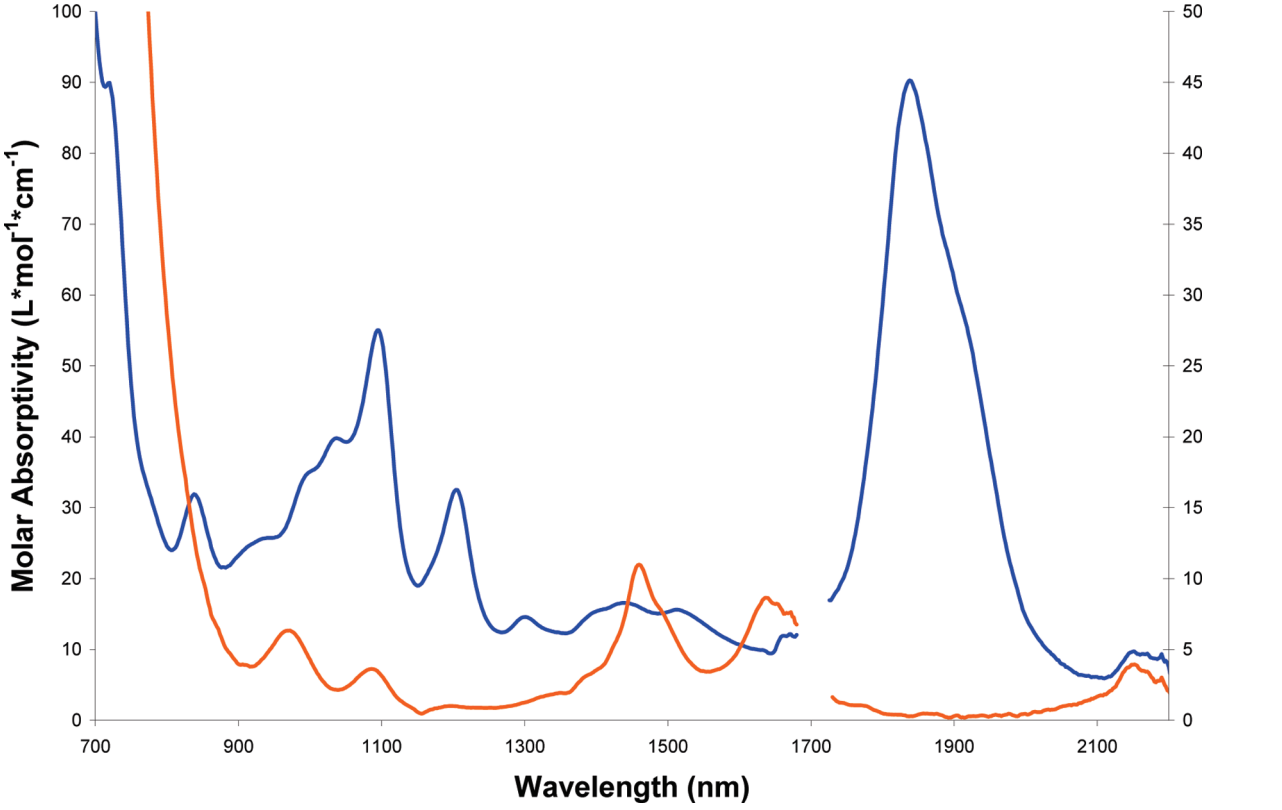

Figure 2. UV−vis/NIR spectrum of **1** (CH_2Cl_2, 4.34 × 10^{-3} M, orange line, right axis) and **3** (CH_2Cl_2, 3.13 × 10^{-3} M, blue line, left axis). Solvent absorption has been removed for clarity.

dx.doi.org/10.1021/ic201385h |*Inorg. Chem.* 2011, 50, 9642–9649

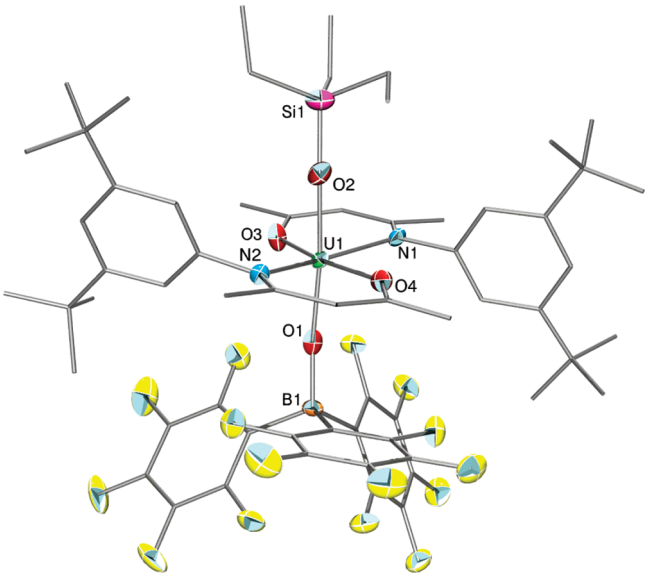

Figure 3. Solid-state structure of $U(OSiEt_3)(OB\{C_6F_5\}_3)(^{Ar}acnac)_2$ (**2**) with 50% probability ellipsoids for the noncarbon atoms. The phenyl rings on the ^{Ar}acnac backbone have been removed for clarity.

of this sample also reveals formation of H_2, observed as a sharp singlet at 4.46 ppm.[47] Formation of H_2 was also observed in the synthesis of $U(OSiPh_3)(OB\{C_6F_5\}_3)(^{Ar}acnac)_2$, where Ph_3SiH was ultimately determined to be the source of the H_2.[23] We also monitored the reaction of $UO_2(^{Ar}acnac)_2$ with only 1 equiv of $HSiEt_3$ in the presence of 1 equiv of $B(C_6F_5)_3$. Under these conditions, complex **1** is still the dominant product but significant amounts of unreacted $UO_2(^{Ar}acnac)_2$ remain in the reaction mixture (Figures S23 and 24, Supporting Information).

Complex **2** can be made on a preparative scale by heating equimolar amounts of $UO_2(^{Ar}acnac)_2$, $HSiEt_3$, and $B(C_6F_5)_3$ in toluene at 85 °C for 5 h. Removal of toluene in vacuo, followed by a hexane extraction and storage at −25 °C for 5 days, results in deposition of a dark amber microcrystalline material in low yield. Surprisingly, thermolysis of **1** in toluene-d_8 at 85 °C for 24 h also results in formation of **2**, concomitant with production of Et_3SiH (Scheme 1), demonstrating that **2** can be formed directly from **1** (Figures S14−S15, Supporting Information). However, conversion to **2** under these conditions is not clean, and several unidentified decomposition products are also observed in the ^{1}H and ^{19}F NMR spectra. We also thermolyzed complex **1** at 50 °C in toluene-d_8; however, very little conversion to **2** was observed at this temperature.

Complex **2** crystallizes in the triclinic space group $P\bar{1}$ (Figure 3). Its U−O_{Si} and U−O_B bond lengths are 2.017(6) and 1.957(6) Å, respectively (Table 1). These parameters are identical to those exhibited by $U(OSiPh_3)(OB\{C_6F_5\}_3)(^{Ar}acnac)_2$.[23] In addition, the U−O_{acnac} bond lengths in **2** are 2.165(7) and 2.198(6) Å, while the U−N bond lengths are 2.440(7) and 2.446(7) Å. As observed for **1**, the ^{1}H and ^{19}F NMR spectra for **2** reveal the presence of two isomers in solution in a 5:1 ratio. For example, the ^{19}F NMR spectrum in CD_2Cl_2 reveals resonances for the ortho, para, and meta fluorines of the major isomer at −78.07, −97.28, and −101.41 ppm, respectively, while the resonances for the para and meta fluorines of the minor isomer are observed at −97.80 and −101.98 ppm. The ortho resonance of the minor isomer is not observed, most likely due to overlap with the corresponding resonance from the major isomer.

To gather further insight into formation of **1**, we monitored the reaction between $UO_2(^{Ar}acnac)_2$, 2 equiv of $DSiEt_3$, and $B(C_6F_5)_3$ in C_6H_6 by ^{2}H NMR spectroscopy. As anticipated, the ^{2}H NMR spectrum of the reaction mixture reveals the presence of $[DB(C_6F_5)_3]^-$, which appears as a broad singlet at 4.64 ppm.[40] This observation is consistent with hydride transfer from silane to $B(C_6F_5)_3$ via the $[Et_3SiH\cdots B(C_6F_5)_3]$ adduct during the course of the reaction. Also observed in the ^{2}H NMR spectrum is a singlet at 3.90 ppm, assignable to unreacted $DSiEt_3$, and a resonance at 3.60 ppm, which could not be assigned (Figure S20, Supporting Information). We do not observe a resonance attributable to D_2 in this spectrum, but this could be due to overlap with the broad $[DB(C_6F_5)_3]^-$ signal.

Generation of both **1** and **2** during the reductive silylation of $UO_2(^{Ar}acnac)_2$ suggests the presence of a common intermediate in their formation, namely, $U^VO(OSiEt_3)(^{Ar}acnac)_2$. The unfunctionalized oxo ligand of this proposed U(V) intermediate could attack either $[Et_3SiH\cdots B(C_6F_5)_3]$ or $B(C_6F_5)_3$ to provide the observed products **1** or **2**, respectively. The observed 4:1 ratio of complex **1** to **2** suggests that silylation of $UO(OSiEt_3)(^{Ar}acnac)_2$ with $[Et_3SiH\cdots B(C_6F_5)_3]$ outcompetes coordination by free $B(C_6F_5)_3$. In contrast, when Ph_3SiH is used in place of Et_3SiH, only one product is observed, namely, $U(OSiPh_3)(OB\{C_6F_5\}_3)(^{Ar}acnac)_2$.[23] To account for the effect of the silane substituents on the reaction outcome, silylation of $U^VO(OSiR_3)(^{Ar}acnac)_2$ by $[Ph_3SiH\cdots B(C_6F_5)_3]$ must be slower than silylation by $[Et_3SiH\cdots B(C_6F_5)_3]$, a hypothesis that fits with the previously measured rate constants of hydride transfer from Et_3SiH and Ph_3SiH.[48,49] It should also be noted that complex **1** is not likely the preferred thermodynamic product, as evidenced by the conversion of **1** to **2** upon thermolysis. That said, direct conversion of **1** to **2** is probably not an important pathway during the room-temperature reaction of $UO_2(^{Ar}acnac)_2$ with Et_3SiH and $B(C_6F_5)_3$, as complex **2** could only be formed directly from **1** at elevated temperatures. Finally, addition of $HSiEt_3$ and $B(C_6F_5)_3$ to **2** at room temperature does not lead to any reaction (Figures S21 and S22, Supporting Information). As a result, the reverse reaction (conversion of **2** into **1**) can also be ruled out.

We also measured the solution-phase redox properties of **1** by cyclic voltammetry. The resulting cyclic voltammogram reveals a quasi-reversible redox feature at −0.37 V (vs Fc/Fc^+), which we attribute to the U(V)/U(IV) redox couple (Figure S30, Supporting Information). This potential is 0.35 V less negative than that observed for $U(OSiPh_3)(OB\{C_6F_5\}_3)(^{Ar}acnac)_2$[23] and 0.84 V less negative than that seen for $[Cp^*_2Co][U(OB\{C_6F_5\}_3)_2(^{Ar}acnac)_2]$.[46] This increase is consistent with positive charge present in $[U(OSiEt_3)_2(^{Ar}acnac)_2]^+$, in contrast to the neutral charge of $U(OSiPh_3)(OB\{C_6F_5\}_3)(^{Ar}acnac)_2$ or the anionic charge of $[U(OB\{C_6F_5\}_3)_2(^{Ar}acnac)_2]^-$.

Reduction of **1** with 1 equiv of Cp_2Co in Et_2O results in precipitation of a yellow-green solid and formation of an orange-red solution. Filtration of this solution, followed by crystallization from Et_2O/hexane, results in the deposition of $U(OSiEt_3)_2(^{Ar}acnac)_2$ (**3**) as an orange-brown crystalline solid in 61% yield (Scheme 1). Dissolution of the yellow-green solid in THF, followed by removal of the volatiles in vacuo, provides $[Cp_2Co][HB(C_6F_5)_3]$ (**4**) as a yellow-green powder in 71% yield.

The room-temperature ^{1}H NMR spectrum of **3** in CD_2Cl_2 is uninformative, but upon cooling to −60 °C, the signals sharpen considerably, revealing two sets of resonances that we attribute to two isomers present in a 1.6:1 ratio. The minor isomer exhibits two inequivalent ^{t}Bu resonances located at −1.12 and −1.55 ppm, while

dx.doi.org/10.1021/ic201385h |*Inorg. Chem.* 2011, 50, 9642–9649

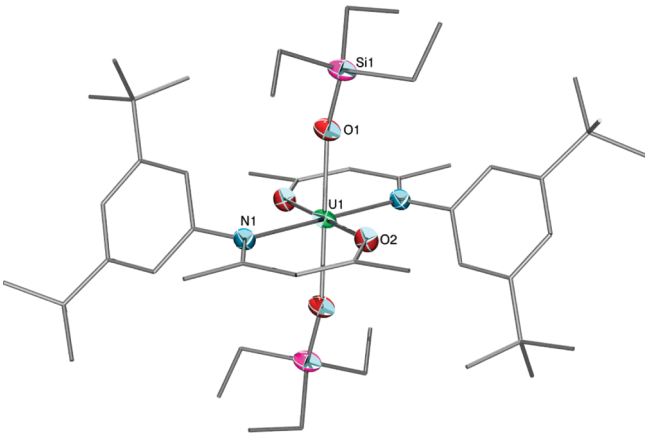

Figure 4. Solid-state structure of $U(OSiEt_3)_2(^{Ar}acnac)_2$ (**3**) with 50% probability ellipsoids for the noncarbon atoms. The phenyl rings on the ^{Ar}acnac backbone have been removed for clarity.

the major isomer exhibits a single ^{t}Bu resonance at −4.48 ppm. In addition, the NIR spectrum for **3** is consistent with reduction to U(IV) and the presence of a $5f^2$ ion (Figure 2).[50,51] The ^{1}H NMR of **4** in CD_2Cl_2 exhibits a singlet at 5.66 ppm, assignable to the cyclopentadienyl resonance of $[Cp_2Co]^+$, and a quartet at 3.64 ppm (J_{BH} = 91 Hz), corresponding to the $[HB(C_6F_5)_3]^-$ resonance.

Complex **3** crystallizes in the monoclinic space group $P2_1/n$, and its solid state molecular structure is shown in Figure 4. Complex **3** is isostructural with complex **1**; however, there are important differences in their metrical parameters (Table 1). The U−O_{Si} bond length in **3** (U1−O1 = 2.129(2) Å) is longer than that observed in **1** but is similar to the U−O bonds in other U(IV) silyloxides,[22] such as $[Cp_2Co][U(OSiPh_3)(OB\{C_6F_5\}_3)(^{Ar}acnac)_2]$ (2.173(8) Å)[23] and $Cp_3U(OSiPh_3)$ (2.135(8) Å).[52] Likewise, the U−N (2.484(3) Å) and U−O_{acnac} (2.268(2) Å) bond lengths in **3** are longer than those observed in **1**, consistent with the presence of the larger U^{4+} ion.

SUMMARY

Reaction of $UO_2(^{Ar}acnac)_2$ with 2 equiv of Et_3SiH in the presence of 1 equiv of $B(C_6F_5)_3$ results in silylation of both oxo ligands and formation of $[U(OSiEt_3)_2(^{Ar}acnac)_2][HB(C_6F_5)_3]$. The presence of the borohydride anion in this material, along with the observed ^{2}H incorporation into the borohydride upon substitution of Et_3SiH with Et_3SiD, provides strong evidence for the intermediacy of a borane−silane adduct, $[Et_3SiH\cdots B(C_6F_5)_3]$, during this transformation.[29−31] This adduct promotes nucleophilic attack on the silyl cation by the uranyl oxo ligand. Interestingly, a second product is also observed in small amounts in the reaction mixture, namely, $U(OSiEt_3)(OB\{C_6F_5\}_3)(^{Ar}acnac)_2$, the product derived from monosilylation of $UO_2(^{Ar}acnac)_2$. The observation of two products in the reaction can be rationalized by formation of a common intermediate, $U^{V}O(OSiEt_3)(^{Ar}acnac)_2$, while the relative ratio of the two products suggests that reaction of $UO(OSiEt_3)(^{Ar}acnac)_2$ with $[Et_3SiH\cdots B(C_6F_5)_3]$ is faster than its reaction with $B(C_6F_5)_3$, resulting in preferential formation of $[U(OSiEt_3)_2(^{Ar}acnac)_2][HB(C_6F_5)_3]$. In addition, reduction of $[U(OSiEt_3)_2(^{Ar}acnac)_2][HB(C_6F_5)_3]$ leads to generation of a neutral U(IV) silyloxide, $U(OSiEt_3)_2(^{Ar}acnac)_2$. This complex appears well poised for selective cleavage of the U−O bond via protonation, which, if achieved, would represent the first well-defined, stepwise cleavage of a uranyl-derived U−O bond. We are currently investigating the feasibility of this transformation.

EXPERIMENTAL SECTION

General. All reactions and subsequent manipulations were performed under anaerobic and anhydrous conditions under an atmosphere of nitrogen or argon. THF, hexanes, diethyl ether, and toluene were dried using a Vacuum Atmospheres DRI-SOLV solvent purification system. Toluene-d_8, C_6H_6, and C_6D_6 were dried over activated 4 Å molecular sieves for 24 h before use. CH_2Cl_2 and CD_2Cl_2 were dried over activated 3 Å molecular sieves for 24 h before use. $UO_2(^{Ar}acnac)_2$ and $(^{Ar}acnac)H$ (Ar = 3,5-^{t}Bu$_2$C$_6$H$_3$) were synthesized according to previously reported procedures.[53] $B(C_6F_5)_3$ was made by the published procedure, except that pentafluoroiodobenzene was used in place of pentafluorobromobenzene.[54] Cp_2Co was recrystallized before use, while all other reagent were purchased from commercial suppliers and used as received.

NMR spectra were recorded on a Varian UNITY INOVA 400 or Varian UNITY INOVA 500 spectrometer. ^{1}H NMR spectra were referenced to external $SiMe_4$ using the residual protio solvent peaks as internal standards. $^{19}F\{^1H\}$ NMR spectra were referenced to external 0.05% α,α,α-trifluorotoluene in C_6D_6. IR spectra were recorded on a Mattson Genesis FTIR spectrometer, while UV−vis/NIR experiments were performed on a UV-3600 Shimadzu spectrophotometer. Elemental analyses were performed by the Microanalytical Laboratory at UC Berkeley.

Cyclic Voltammetry Measurements. CV experiments were performed with a CH Instruments 600c Potentiostat, and the data were processed using CHI software (version 6.29). All experiments were performed in a glovebox using a 20 mL glass vial as the cell. The working electrode consisted of a platinum disk embedded in glass (2 mm diameter), while platinum wire was used for both counter and reference electrodes. Solutions employed during CV studies were typically 3 mM in the uranium complex and 0.1 M in $[Bu_4N][PF_6]$. All potentials are reported versus the $[Cp_2Fe]^{0/+}$ couple. For all trials, $i_{p,a}/i_{p,c}$ = 1 for the $[Cp_2Fe]^{0/+}$ couple, while $i_{p,c}$ increased linearly with the square root of the scan rate (i.e., $\sqrt{v}$).

$[U(OSiEt_3)_2(^{Ar}acnac)_2][HB(C_6F_5)_3]$ (Ar = 3,5-^{t}Bu$_2$C$_6$H$_3$) (1). To a red dichloromethane (3 mL) solution of $UO_2(^{Ar}acnac)_2$ (167 mg, 0.153 mmol) was added $HSiEt_3$ (49 μL, 0.31 mmol) and $B(C_6F_5)_3$ (80 mg, 0.16 mmol), resulting in formation of a dark amber solution. After stirring for 6 h, the deep red solution was filtered through a Celite column supported on glass wool (0.5 cm × 2 cm). The solution was then concentrated in vacuo, layered with hexanes, and stored at −25 °C for 24 h, producing a dark red crystalline material (225 mg, 80% yield). Anal. Calcd for $UO_4N_2Si_2BF_{15}C_{88}H_{95}$: C, 57.61; H, 5.22; N, 1.53. Found: C, 57.98; H, 5.26; N, 1.76. ^{1}H NMR (CD_2Cl_2, 25 °C, 500 MHz, trans isomer): δ 7.32 (t, 2H, J_{HH} = 6.8 Hz, para CH), 6.95 (t, 2H, J_{HH} = 7.0 Hz, para CH), 6.70 (d, 4H, J_{HH} = 6.6 Hz, meta CH), 6.64 (d, 4H, meta CH), 6.04 (br s, 4H, ortho CH), 5.46 (br s, 12H, three overlapping resonances attributable to the ortho CH, CH_2CH_3, and para N-aryl CH), 4.85 (br s, 6H, CH_2CH_3), 4.06 (s, 2H, γ-CH), 3.29 (s, 18H, CH_2CH_3), −0.05 (s, 36H, CMe_3). The $HB(C_6F_5)_3$ resonance was not observed, most likely due to overlap with the CH_2CH_3 resonance at 3.29 ppm. Also, the two ortho N-aryl CH resonances were not observed, possibly due to paramagnetic broadening. ^{1}H NMR (CD_2Cl_2, 25 °C, 500 MHz, cis isomer): δ 9.61 (br s), 8.02 (s), 7.95 (s), 1.55 (br s), −0.40 (s, CMe_3), −1.18 (br s). The remaining resonances assignable to the cis isomer were not observed. $^{19}F\{^1H\}$ NMR (CD_2Cl_2, 25 °C, 470 MHz): δ −69.80 (d, 6F, J_{FF} = 19.7 Hz, ortho CF), −100.63 (t, 3F, J_{FF} = 20.2 Hz, para CF), −103.46 (t, 6F, J_{FF} = 19.0 Hz, meta CF). ^{1}H NMR (CD_2Cl_2, 12 °C, 500 MHz, trans isomer): δ 7.30 (t, 2H, J_{HH} = 6.8 Hz, para CH), 6.94 (t, 2H, J_{HH} = 7.2 Hz, para CH), 6.68 (d, 4H, J_{HH} = 6.6 Hz, meta CH), 6.61 (s, 4H, meta CH), 5.99 (br s, 4H, ortho CH), 5.64 (br s, 6H, CH_2CH_3), 5.44 (br s, 2H, para N-aryl CH), 5.20 (br s, 4H, ortho CH), 4.98 (br s, 6H, CH_2CH_3), 3.91 (s, 2H, γ-CH), 3.39 (s, 18H, CH_2CH_3), −0.10 (s, 36H, CMe_3). The $HB(C_6F_5)_3$ resonance was not observed, most likely due to overlap with the CH_2CH_3 resonance at 3.39 ppm.

dx.doi.org/10.1021/ic201385h |*Inorg. Chem.* 2011, 50, 9642–9649

Also, the two ortho N-aryl CH resonances were not observed, possibly due to paramagnetic broadening. ^{1}H NMR (CD_2Cl_2, 12 °C, 500 MHz, cis isomer): δ 1.54 (br s), −0.42 (s, CMe_3), −0.48 (s, CMe_3), −1.43 (br s). The remaining resonances assignable to the cis isomer were not observed. UV−vis/NIR (CH_2Cl_2, 4.34×10^{-3} M, L·mol^{-1}·cm^{-1}): 850 (sh, ε = 10), 980 (ε = 6), 1090 (ε = 3), 1210 (ε = 1), 1350 (ε = 2), 1400 (sh, ε = 3), 1430 (sh, ε = 6), 1460 (ε = 11), 1490 (ε = 8), 1640 (ε = 8), 1670 (ε = 7), 1780 (ε = 2), 2150 (ε = 8), 2170 (sh, ε = 7), 2190 nm (ε = 6). IR (KBr pellet, cm^{-1}): 3102(sh w), 3086(sh w), 3068(w), 3033(w), 2965(vs), 2940(sh s), 2911(s), 2879(s), 2377(w, ν_{BH}), 2359(w), 1660(w), 1640(m), 1594(s), 1586(s), 1556(vs), 1508(vs), 1467(vs), 1455(sh vs), 1439(vs), 1413(sh s), 1396(s), 1363(s), 1337(sh m), 1314(m), 1293(vs), 1277(s), 1244(s), 1240(sh s), 1205(w), 1182(w), 1161(w), 1127(sh m), 1114(s) 1101(s), 1078(s), 1065(s), 1024(s), 1000(m), 969(vs), 919(sh m), 900(s), 890(s), 874(m), 812(vs), 808(vs), 786(s), 771(s), 765(sh s), 748(s), 740(sh s), 712(s), 698(s), 694(sh s), 673(m), 659(m), 644(sh m), 618(w), 601(m), 581(s), 566(m), 548(m), 531(m), 503(m), 494(sh m), 462(m), 446(m), 432(m).

U(OSiEt$_3$)(OB{C$_6$F$_5$}$_3$)(^{Ar}acnac)$_2$ (Ar = 3,5-^{t}Bu$_2$C$_6$H$_3$) (2). A reaction flask was charged with a toluene (3.5 mL) solution containing $UO_2(^{Ar}acnac)_2$ (84 mg, 0.077 mmol), $HSiEt_3$ (12 μL, 0.075 mmol), and $B(C_6F_5)_3$ (40 mg, 0.078 mmol). The flask was sealed, and the solution was heated at 85 °C for 5.25 h. The volatiles were removed in vacuo, and hexanes (4 mL) was added, resulting in formation of dark precipitate. The solution was filtered through a Celite column supported on glass wool (0.5 cm × 2 cm) and concentrated in vacuo (2 mL). Storage at −25 °C for 5 days resulted in formation of a dark amber microcrystalline material (23 mg, 18% yield), which was washed with hexane (2 × 1 mL). Anal. Calcd for $UO_4N_2SiBF_{15}C_{82}H_{79}\cdot C_6H_{14}$: C, 58.57; H, 5.19; N, 1.55. Found: C, 58.30; H, 5.05; N, 1.56. ^{1}H NMR (C_6D_6, 25 °C, 500 MHz, trans isomer): δ 6.93 (t, 2H, J_{HH} = 7.2 Hz, para CH), 6.44 (t, 2H, J_{HH} = 7.1 Hz, para CH), 6.42 (d, 4H, J_{HH} = 7.2 Hz, meta CH), 6.27 (s, 4H, meta CH), 6.09 (br s, 4H, ortho CH), 5.23 (br s, 6H, overlapping ortho CH and para N-aryl CH), 4.94 (br s, 3H, CH_2CH_3), 4.69 (br s, 5H, overlapping CH_2CH_3 and γ-CH), 3.41 (br s, 9H, CH_2CH_3), 0.20 (br s, 18H, CMe_3), 0.02 (br s, 18H, CMe_3). The two ortho N-aryl CH resonances were not observed. ^{1}H NMR (C_6D_6, 25 °C, 500 MHz, cis isomer): δ 2.16, −0.48 (s, CMe_3), −0.58 (s, CMe_3), −0.92 (s, CMe_3), −1.03 (s, CMe_3). The remaining resonances assignable to the cis isomer were not observed. ^{19}F{^{1}H} NMR (C_6D_6, 25 °C, 470 MHz): δ −77.83 (br s, ortho CF, trans isomer), −95.81 (t, 3F, J_{FF} = 18.5 Hz, para CF, trans isomer), −96.37 (s, 3F, para CF, cis isomer), −100.43 (d, 6F, J_{FF} = 18.9 Hz, meta CF, trans isomer), −100.90 (s, 6F, meta CF, cis isomer). The ortho fluorine resonance for the cis isomer was not observed, possibly due to overlap with the resonance for the trans isomer. ^{1}H NMR (CD_2Cl_2, 25 °C, 500 MHz, trans isomer): δ 7.19 (t, 2H, J_{HH} = 6.8 Hz, para CH), 6.82 (t, 2H, J_{HH} = 6.9 Hz, para CH), 6.58 (d, 4H, J_{HH} = 6.0 Hz, meta CH), 6.54 (s, 4H, meta CH), 5.96 (br s, 4H, ortho CH), 5.19 (br s, 4H, ortho CH), 5.10 (br s, 2H, para N-aryl CH), 4.91 (br s, 3H, CH_2CH_3), 4.64 (br s, 3H, CH_2CH_3), 4.59 (s, 2H, γ-CH), 3.35 (br s, 9H, CH_2CH_3), 0.13 (br s, 18H, CCH_3), −0.11 (br s, 18H, CCH_3). The two ortho N-aryl CH resonances were not observed. ^{1}H NMR (CD_2Cl_2, 25 °C, 500 MHz, cis isomer): δ 10.44, 8.64, 8.17, 8.01, 7.52, 7.44, 2.02, −0.63 (s, CMe_3), −0.76 (s, CMe_3), −0.85 (s, CMe_3), −0.96 (s, CMe_3). The remaining resonances assignable to the cis isomer were not observed. ^{19}F{^{1}H} NMR (CD_2Cl_2, 25 °C, 470 MHz): δ −78.07 (br s, ortho CF, trans isomer), −97.28 (t, 3F, J_{FF} = 18.8 Hz, para CF, trans isomer), −97.80 (s, 3F, para CF, cis isomer), −101.41 (d, 6F, J_{FF} = 18.4 Hz, meta CF, trans isomer), −101.98 (s, 6F, meta CF, cis isomer). The ortho CF resonance for the cis isomer is not observed. ^{1}H NMR (CD_2Cl_2, −15 °C, 500 MHz, trans isomer): δ 7.14 (s, 2H, para CH), 6.77 (s, 2H, para CH), 6.44 (s, 8H, overlapping meta CH resonances), 5.77 (br s, 4H, ortho CH), 5.60 (br s, 3H, CH_2CH_3), 5.22 (br s, 3H, CH_2CH_3), 4.99 (br s, 2H, para N-aryl CH), 4.75 (br s, 4H, ortho CH), 4.20 (s, 2H, γ-CH), 3.74 (br s, 9H, CH_2CH_3), 0.04 (s, 18H, CMe_3), −0.40 (s, 18H, CMe_3). The two ortho N-aryl CH resonances were not observed. ^{1}H NMR (CD_2Cl_2, −15 °C, 500 MHz, cis isomer): δ 2.01, −0.77 (s, CMe_3), −0.91 (s, CMe_3), −1.25 (s, CMe_3), −1.38 (s, CMe_3), −2.48. The remaining resonances assignable to the cis isomer were not observed. IR (KBr pellet, cm^{-1}): 2964(s), 2940(sh m), 2921(sh m), 2874(m), 1641(m), 1596(m), 1586(m), 1559(vs), 1539(sh m), 1514(vs), 1485(sh vs), 1471(vs), 1451(sh vs), 1440(vs), 1424(sh m), 1394(m), 1393(m), 1364(m), 1313(sh m), 1293(s), 1280(s), 1247(m), 1241(sh m), 1204(w), 1182(w), 1158(w), 1130(w), 1120(w), 1096(sh s), 1085(s), 1065(m), 1024(m), 999(m), 980(s), 936(sh w), 926(w), 920(w), 900(m), 890(m), 873(m), 870(sh m), 838(s), 817(vs), 784(m), 772(s), 763(m), 759(sh m), 750(m), 735(m), 733(sh m) 708(m), 698(s), 687(m), 683(m), 670(m), 659(w), 654(w), 633(w), 617(w), 605(w), 578(m), 547(w), 525(w), 503(w), 491(w), 480(w), 460(w), 437(w), 423(sh w), 414(w).

U(OSiEt$_3$)$_2$(^{Ar}acnac)$_2$ (Ar = 3,5-^{t}Bu$_2$C$_6$H$_3$) (3). To a red Et_2O (3 mL) suspension of $[U(OSiEt_3)_2(^{Ar}acnac)_2][HB(C_6F_5)_3]$ (**1**) (192 mg, 0.105 mmol) was added an Et_2O (1 mL) solution of Cp_2Co (20 mg, 0.11 mmol). This resulted in formation of a red solution and a yellow-green precipitate. The mixture was stirred for 1.5 h before being filtered through a Celite column supported on glass wool (0.5 cm × 2 cm), producing an orange-red supernatant and yellow-green plug. The supernatant was concentrated in vacuo, layered with hexanes, and stored at −25 °C for 48 h, producing a dark red crystalline material (84 mg, 61% yield). Anal. Calcd for $UO_4N_2Si_2C_{70}H_{94}$: C, 63.61; H, 7.17; N, 2.12. Found: C, 63.53; H, 4.42; N, 1.48. ^{1}H NMR (CD_2Cl_2, −60 °C, 500 MHz, cis isomer): δ 14.85 (s, 2H, para N-aryl CH), 13.36 (s, 4H, meta CH), 10.01 (s, 2H, para CH), 8.13 (s, 4H, meta CH), 7.70 (s, 2H, para CH), 6.68 (br s, 4H, ortho CH), 3.73 (s, 2H, γ-CH), 0.98 (s, 4H, ortho CH), 0.85 (s, 18H, CH_2CH_3), 0.16 (s, 6H, CH_2CH_3), −1.12 (s, 18H, CMe_3), −1.55 (s, 18H, CMe_3), −9.22 (br s, 2H, ortho N-aryl CH), −10.67 (br s, 2H, ortho N-aryl CH). One of the CH_2CH_3 resonances was not observed, possibly due to overlap with another resonance. ^{1}H NMR (CD_2Cl_2, −60 °C, 500 MHz, trans isomer): δ 53.53 (br s, 6H, CH_2CH_3), 52.17 (br s, 6H, CH_2CH_3), 27.98 (br s, 18H, CH_2CH_3), 1.45 (s, 2H), −1.98 (s, 4H), −4.48 (s, 36H, CMe_3), −4.61 (s, 4H), −7.96 (br s, 2H), −12.02 (br s, 4H), −21.67 (br s, 4H), −26.14 (br s, 4H), −32.14 (br s, 2H). One resonance integrating for 2 protons was not observed. UV−vis/NIR (CH_2Cl_2, 3.13×10^{-3} M, L·mol^{-1}·cm^{-1}): 720 (ε = 90), 760 (sh, ε = 36), 840 (ε = 32), 940 (ε = 26), 1010 (sh, ε = 35), 1040 (ε = 40), 1100 (ε = 55), 1210 (ε = 32), 1310 (ε = 14), 1410 (sh, ε = 16), 1450 (ε = 16), 1520 (ε = 16), 1640 (ε = 10), 1670 (ε = 12), 1840 (ε = 90), 1890 (sh, ε = 65), 2160 nm (ε = 9). IR (KBr pellet, cm^{-1}): 3104(w), 3083(w), 3063(w), 3029(w), 2958(vs), 2905(s), 2873(s), 2804(w), 1587(s), 1563(sh s), 1555(vs), 1494(vs), 1484(vs), 1479(vs), 1467(vs), 1457(vs), 1440(vs), 1421(s), 1389(vs), 1368(s), 1348(sh m), 1313(s), 1296(s), 1282(sh s), 1268(sh m), 1240(s), 1205(m), 1180(w), 1157(w), 1133(w), 1128(sh w), 1106(w), 1078(m), 1065(m), 1024(m), 1004(m), 984(m), 973(m), 965(m), 937(m), 931(m), 898(sh s), 885(vs), 846(sh m), 825(sh m), 803(w), 781(m), 767(sh s), 761(s), 736(s), 712(s), 694(s), 671(m), 664(sh m), 651(sh w), 643(sh w), 639(sh w), 617(w), 607(m), 575(m), 566(m), 546(w), 523(w), 495(m), 460(sh w), 444(m), 439(m).

[Cp$_2$Co][HB(C$_6$F$_5$)$_3$] (4). The yellow-green solid generated during the synthesis of complex **3** was dissolved in THF (2 mL) and filtered through a Celite column supported on glass wool (0.5 cm × 2 cm). The volatiles were removed in vacuo, and the resulting solid was washed with hexanes (3 mL) and Et_2O (3 mL) and subsequently dried in vacuo yielding $[Cp_2Co][HB(C_6F_5)_3]$ as a yellow-green powder (54 mg, 71% yield). ^{1}H NMR (CD_2Cl_2, 25 °C, 500 MHz): δ 5.66 (s, 10H, CH), 3.64 (br quartet, 1H, J_{BH} = 90.8 Hz, BH). ^{19}F{^{1}H} NMR (CD_2Cl_2, 25 °C, 470 MHz): δ −69.66 (d, 6F, J_{FF} = 20.9 Hz, ortho CF), −100.06 (t, 3F, J_{FF} = 20.1 Hz, para CF), −103.08 (t, 6F, J_{FF} = 18.9 Hz, meta CF).

NMR-Scale Synthesis of 1 Using DSiEt$_3$. A red C_6H_6 solution (1 mL) containing $UO_2(^{Ar}acnac)_2$ (23 mg, 0.021 mmol) and $DSiEt_3$ (6.7 μL, 0.042 mmol) was sealed in a J Young NMR tube, and the ^{2}H

dx.doi.org/10.1021/ic201385h |Inorg. Chem. 2011, 50, 9642–9649

Table 2. X-ray Crystallographic Data for Complexes 1−3

	1	2	3
empirical formula	$UO_4N_2Si_2BF_{15}C_{88}H_{95}$	$UO_4N_2SiBF_{15}C_{82}H_{79}$	$UO_4N_2Si_2C_{70}H_{94}$
crystal habit, color	plate, dark orange	plate, dark red	irregular, dark red
cryst size (mm)	0.54 × 0.34 × 0.16	0.20 × 0.18 × 0.10	0.40 × 0.28 × 0.22
cryst syst	triclinic	triclinic	monoclinic
space group	*P*-1	*P*-1	$P2_1/n$
volume (Å^3)	4238.0(10)	3730(2)	3368.7(3)
a (Å)	13.1761(18)	12.909(4)	12.6522(8)
b (Å)	17.822(3)	16.329(5)	17.5193(10)
c (Å)	20.054(3)	19.010(6)	15.3466(9)
α (deg)	98.520(2)	78.273(5)	90
β (deg)	102.891(2)	87.803(5)	97.991(2)
γ (deg)	108.220(2)	71.991(6)	90
Z	2	2	2
fw (g/mol)	1834.68	1718.40	1321.68
density(calcd) (Mg/m^3)	1.438	1.530	1.303
abs coeff (mm^{-1})	2.026	2.282	2.491
F_{000}	1858	1726	1360
total no. reflns	32 304	28 620	26 773
unique reflns	15 837	13 512	6764
final *R* indices [$I > 2\sigma(I)$]	R_1 = 0.0470	R_1 = 0.0783	R_1 = 0.0269
	wR_2 = 0.1039	wR_2 = 0.1370	wR_2 = 0.0661
largest diff. peak and hole (e$^-$ Å^{-3})	1.499 and −2.673	4.556 and −2.566	0.808 and −0.925
GOF	0.959	1.126	0.950

NMR spectrum was obtained. The solution was then frozen, whereupon a C_6H_6 solution (1 mL) of $B(C_6F_5)_3$ (10 mg, 0.021 mmol) was layered onto the frozen plug. The tube was sealed, and the reaction was initiated by thawing the frozen plug, resulting in a deep red solution. The reaction was allowed to proceed for 19 h before the ^{2}H NMR spectrum was collected (Figures S19−S20, Supporting Information). ^{2}H NMR (C_6H_6, 25 °C, 77 MHz): δ 4.64 (br s, $[DB(C_6F_5)_3]$), 3.90 (s, $DSiEt_3$), 3.60 (s).

NMR-Scale Synthesis of 1 Using $HSiEt_3$. A C_6D_6 solution (1 mL) containing $UO_2(^{Ar}acnac)_2$ (21 mg, 0.019 mmol) and $HSiEt_3$ (6.1 μL, 0.038 mmol) was sealed in a J Young NMR tube, and the ^{1}H NMR spectrum was obtained. The solution was then frozen, whereupon a C_6D_6 solution (1 mL) of $B(C_6F_5)_3$ (10 mg, 0.021 mmol) was layered onto the frozen plug. The tube was sealed, and the reaction was initiated by thawing the frozen plug, resulting in a deep red solution. The reaction was allowed to proceed for 21 h before the ^{1}H and ^{19}F NMR spectra were collected (Figures S17−S18, Supporting Information).

NMR-Scale Synthesis of 1 Using 1 Equiv of $HSiEt_3$. A red C_6D_6 solution (0.5 mL) containing $UO_2(^{Ar}acnac)_2$ (14 mg, 0.013 mmol) and $HSiEt_3$ (2.1 μL, 0.013 mmol) was sealed in a J Young NMR tube, and the ^{1}H NMR spectrum was obtained. The solution was then frozen, whereupon a C_6D_6 solution (0.5 mL) of $B(C_6F_5)_3$ (7 mg, 0.013 mmol) was layered onto the frozen plug. The tube was sealed, and the reaction was initiated by thawing the frozen plug, resulting in a deep red solution. The reaction was allowed to proceed for 2 h before the ^{1}H and ^{19}F NMR spectra were collected (Figures S23 and S24, Supporting Information).

NMR-Scale Thermolysis of 1 in Tol-d_8. Complex **1** (10 mg, 0.005 mmol) was dissolved in toluene-d_8 (0.73 mL) and heated at 85 °C for 23 h, resulting in a color change to dark amber. The ^{1}H and ^{19}F NMR spectra revealed a decrease in the resonances assignable to **1** and the presence of new resonances attributable to **2** as well as $HSiEt_3$ and other unidentified products (Figures S14−S15, Supporting Information).

X-ray Crystallography. The solid state molecular structures of complexes **1**−**3** were determined similarly with exceptions noted in the following paragraph. Crystals were mounted on a glass fiber under Paratone-N oil. Data collection was carried out on a Bruker 3-axis platform diffractometer with SMART-1000 CCD detector. The instrument was equipped with graphite-monochromatized Mo Kα X-ray source (λ = 0.71073 Å). All data were collected at 150(2) K using an Oxford nitrogen gas cryostream system. A hemisphere of data was collected using ω scans and 0.3° frame widths. Frame exposures of 20, 35, and 20 s were used for complexes **1**, **2**, and **3**, respectively. SMART[55] was used to determine the cell parameters, and the raw frame data were processed using SAINT.[56] The empirical absorption correction was applied based on Psi-scan or SADABS. Subsequent calculations were carried out using SHELXTL.[57] The structures were solved using direct methods and difference Fourier techniques. All hydrogen atom positions were idealized and rode on the atom of attachment. Unless otherwise noted, the final refinement included anisotropic temperature factors on all non-hydrogen atoms. Structure solution, refinement, graphics, and creation of publication materials were performed using SHELXTL.

Complex **1** exhibits positional disorder of the $[HB(C_6F_5)_3]^-$ anion. The positional disorder was addressed by modeling the molecule in two orientations, in a 65:35 ratio. Several carbon atoms within the disordered anion were not refined anisotropically. In addition, the C−C and C−F bonds of the aryl rings were fixed with the DFIX command, while the rings were constrained with the FLAT command. The EADP command was used to constrain C3, C7, C10, C72B, and C73B. An idealized hydrogen atom was not assigned to the disordered $[HB(C_6F_5)_3]^-$ anion in **1**. For complex **2**, C23, C52, C44, C66, and C70 were constrained using the EADP command. A summary of relevant crystallographic data for complexes **1**−**3** is presented in Table 2.

■ ASSOCIATED CONTENT

Supporting Information. Cyclic voltammetry data for complex **1**; crystallographic details (as CIF files); IR spectra for complexes **1**−**3**; ^{1}H and ^{19}F NMR spectra for complexes **1**−**4**. This material is available free of charge via the Internet at http://pubs.acs.org.

dx.doi.org/10.1021/ic201385h |*Inorg. Chem.* 2011, 50, 9642–9649

AUTHOR INFORMATION

Corresponding Author
*E-mail: hayton@chem.ucsb.edu.

ACKNOWLEDGMENT

We thank the University of California, Santa Barbara, and the Department of Energy Basic Energy Sciences program for financial support of this work.

REFERENCES

(1) Fortier, S.; Hayton, T. W. *Coord. Chem. Rev.* **2010**, *254*, 197–214.
(2) Denning, R. G. *J. Phys. Chem. A* **2007**, *111*, 4125–4143.
(3) deB Darwent, B. *Nat. Stand. Ref. Data Ser.* **1970**, *31*, 1–48.
(4) Berthet, J.-C.; Nierlich, M.; Ephritikhine, M. *C. R. Chim.* **2002**, *5*, 81–88.
(5) Berthet, J.-C.; Lance, M.; Nierlich, M.; Ephritikhine, M. *Eur. J. Inorg. Chem.* **2000**, 1969–1973.
(6) Anderson, R. T.; Vrionis, H. A.; Ortiz-Bernad, I.; Resch, C. T.; Long, P. E.; Dayvault, R.; Karp, K.; Marutzky, S.; Metzler, D. R.; Peacock, A.; White, D. C.; Lowe, M.; Lovley, D. R. *Appl. Environ. Microbiol.* **2003**, *69*, 5884–5891.
(7) Choppin, G. R.; Stout, B. E. *Sci. Total Environ.* **1989**, *83*, 203–216.
(8) Choppin, G. R.; Wong, P. J. *Aquat. Geochem.* **1998**, *4*, 77–103.
(9) Konhauser, K. O.; Mortimer, R. J. G.; Morris, K.; Dunn, V. In *Interactions of Microorganisms with Radionuclides*; Keith-Roach, M. J., Livens, F. R., Eds.; Elsevier: Amsterdam, 2002; pp 61−100.
(10) Renshaw, J. C.; Butchins, L. J. C.; Livens, F. R.; May, I.; Charnock, J. M.; Lloyd, J. R. *Environ. Sci. Technol.* **2005**, *39*, 5657–5660.
(11) Runde, W. *Los Alamos Sci.* **2000**, *26*, 392–411.
(12) Arnold, P. L.; Pécharman, A.-F.; Hollis, E.; Yahia, A.; Maron, L.; Parsons, S.; Love, J. B. *Nat. Chem.* **2010**, *2*, 1056–1061.
(13) Arnold, P. L.; Hollis, E.; White, F. J.; Magnani, N.; Caciuffo, R.; Love, J. B. *Angew. Chem., Int. Ed.* **2011**, *50*, 887–890.
(14) Nocton, G.; Horeglad, P.; Vetere, V.; Pecaut, J.; Dubois, L.; Maldivi, P.; Edelstein, N. M.; Mazzanti, M. *J. Am. Chem. Soc.* **2010**, *132*, 495–508.
(15) Nocton, G.; Horeglad, P.; Pecaut, J.; Mazzanti, M. *J. Am. Chem. Soc.* **2008**, *130*, 16633–16645.
(16) Burdet, F.; Pecaut, J.; Mazzanti, M. *J. Am. Chem. Soc.* **2006**, *128*, 16512–16513.
(17) Natrajan, L.; Burdet, F.; Pecaut, J.; Mazzanti, M. *J. Am. Chem. Soc.* **2006**, *128*, 7152–7153.
(18) Mougel, V.; Horeglad, P.; Nocton, G.; Pecaut, J.; Mazzanti, M. *Chem.—Eur. J.* **2010**, *16*, 14365–14377.
(19) Mougel, V.; Biswas, B.; Pecaut, J.; Mazzanti, M. *Chem. Commun.* **2010**, *46*, 8648–8650.
(20) Mougel, V.; Horeglad, P.; Nocton, G.; Pecaut, J.; Mazzanti, M. *Angew. Chem., Int. Ed.* **2009**, *48*, 8477–8480.
(21) Brown, J. L.; Wu, G.; Hayton, T. W. *J. Am. Chem. Soc.* **2010**, *132*, 7248–7249.
(22) Brown, J. L.; Mokhtarzadeh, C. C.; Lever, J. M.; Wu, G.; Hayton, T. W. *Inorg. Chem.* **2011**, *50*, 5105–5112.
(23) Schnaars, D. D.; Wu, G.; Hayton, T. W. *Inorg. Chem.* **2011**, *50*, 4695–4697.
(24) Berthet, J.-C.; Siffredi, G.; Thuéry, P.; Ephritikhine, M. *Eur. J. Inorg. Chem.* **2007**, 4017–4020.
(25) Arnold, P. L.; Patel, D.; Wilson, C.; Love, J. B. *Nature* **2008**, *451*, 315–317.
(26) Arnold, P. L.; Love, J. B.; Patel, D. *Coord. Chem. Rev.* **2009**, *253*, 1973–1978.
(27) Yahia, A.; Arnold, P. L.; Love, J. B.; Maron, L. *Chem. Commun.* **2009**, 2402–2404.
(28) Yahia, A.; Arnold, P. L.; Love, J. B.; Maron, L. *Chem.—Eur. J.* **2010**, *16*, 4881–4888.
(29) Parks, D. J.; Blackwell, J. M.; Piers, W. E. *J. Org. Chem.* **2000**, *65*, 3090–3098.
(30) Parks, D. J.; Piers, W. E. *J. Am. Chem. Soc.* **1996**, *118*, 9440–9441.
(31) Rendler, S.; Oestreich, M. *Angew. Chem., Int. Ed.* **2008**, *47*, 5997–6000.
(32) Bach, P.; Albright, A.; Laali, K. K. *Eur. J. Org. Chem.* **2009**, 1961–1966.
(33) Berkefeld, A.; Piers, W. E.; Parvez, M. *J. Am. Chem. Soc.* **2010**, *132*, 10660–10661.
(34) Blackwell, J. M.; Morrison, D. J.; Piers, W. E. *Tetrahedron* **2002**, *58*, 8247–8254.
(35) Blackwell, J. M.; Sonmor, E. R.; Scoccitti, T.; Piers, W. E. *Org. Lett.* **2000**, *2*, 3921–3923.
(36) Piers, W. E.; Marwitz, A. J. V.; Mercier, L. G. *Inorg. Chem.* **2011**, 50, DOI: 10.1021/ic2006474.
(37) Dagorne, S.; Janowska, I.; Welter, R.; Zakrsewski, J.; Jaouen, G. *Organometallics* **2004**, *23*, 4706–4710.
(38) Holschumacher, D.; Taouss, C.; Bannenberg, T.; Hrib, C. G.; Daniliue, C. G.; Jones, P. G.; Tamm, M. *Dalton Trans.* **2009**, 6927–6929.
(39) Walker, D. A.; Woodman, T. J.; Schormann, M.; Hughes, D. L.; Bochmann, M. *Organometallics* **2003**, *22*, 797–803.
(40) Wang, H.; Fröhlich, R.; Kehr, G.; Erker, G. *Chem. Commun.* **2008**, 5966–5968.
(41) Röttger, D.; Schmuck, S.; Erker, G. *J. Organomet. Chem.* **1996**, *508*, 263–265.
(42) Temme, B.; Erker, G. *J. Organomet. Chem.* **1995**, *488*, 177–182.
(43) Yang, X.; Stern, C. L.; Marks, T. J. *Angew. Chem., Int. Ed.* **1992**, *31*, 1375–1377.
(44) Graves, C. R.; Vaughn, A. E.; Schelter, E. J.; Scott, B. L.; Thompson, J. D.; Morris, D. E.; Kiplinger, J. L. *Inorg. Chem.* **2008**, *47*, 11879–11891.
(45) Ryan, J. L. *J. Inorg. Nucl. Chem.* **1971**, *33*, 153–177.
(46) Schnaars, D. D.; Wu, G.; Hayton, T. W. *J. Am. Chem. Soc.* **2009**, *131*, 17532–17533.
(47) Fulmer, G. R.; Miller, A. J. M.; Sherden, N. H.; Gottlieb, H. E.; Nudelman, A.; Stoltz, B. M.; Bercaw, J. E.; Goldberg, K. I. *Organometallics* **2010**, *29*, 2176–2179.
(48) Carey, F. A.; Tremper, H. S. *J. Am. Chem. Soc.* **1968**, *90*, 2578–2583.
(49) Mayr, H.; Basso, N.; Hagen, G. *J. Am. Chem. Soc.* **1992**, *114*, 3060–3066.
(50) Cohen, D.; Carnall, W. T. *J. Phys. Chem.* **1960**, *64*, 1933–1936.
(51) Monreal, M. J.; Diaconescu, P. L. *Organometallics* **2008**, *27*, 1702–1706.
(52) Porchia, M.; Brianese, N.; Casellato, U.; Ossola, F.; Rossetto, G.; Zanella, P. *J. Chem. Soc., Dalton Trans.* **1989**, 677–681.
(53) Hayton, T. W.; Wu, G. *Inorg. Chem.* **2009**, *48*, 3065–3072.
(54) Chernega, A. N.; Graham, A. J.; Green, M. L. H.; Haggit, J.; Lloyd, J.; Mehnert, C. P.; Metzler, N.; Souter, J. *Dalton Trans.* **1997**, 2293–2303.
(55) *SMART Software Users Guide*, 5.1; Bruker Analytical X-ray Systems, Inc.: Madison, WI, 1999.
(56) *SAINT Software Users Guide*, 5.1; Bruker Analytical X-ray Systems, Inc.: Madison, WI, 1999.
(57) Sheldrick, G. M. *SHELXTL*, 6.12; Bruker Analytical X-ray Systems, Inc.: Madison, WI, 2001.